Supporting Information

Phosphoric acid densified red emissive carbon dots with well-defined structure and narrow band fluorescence for intracellular reactive oxygen species detection and scavenging

Yalan Xu[a], Chan Wang[a], Laizhi Sui[b], Guoxia Ran[a], Qijun Song[a]*

[a] Key Laboratory of Synthetic and Biological Colloids, Ministry of Education, School of Chemical and Material Engineering, Jiangnan University, Wuxi 214122, China.

[b] State Key Laboratory of Molecular Reaction Dynamics, Dalian Institute of Chemical Physics, Chinese Academy of Sciences, Dalian, 116023, China

Materials

Catechol, resorcinol, hydroquinone, phloroglucinol, p-phenylenediamine, o-phenylenediamine, 4-aminophenol, phosphate (H_3PO_4), and microporous membrane (0.22 μm, mixed fiber-water system) were purchased from Sinopharm Chemical Reagent Co., Ltd. Sodium hypochlorite (NaClO), ferrous sulfate ($FeSO_4$), and hydrogen peroxide (H_2O_2), were obtained from Sigma–Aldrich, USA. Xanthine and xanthine oxidase were obtained from Yuanye Co., Ltd. (Shanghai, China). 5, 5-dimethyl-1-pyrroline N-oxide (DMPO) was purchased from Energy Chemical Co. Ltd and stored at 4 ℃. The cytotoxicity detection kit Cell Counting Kit-8 (CCK-8), apoptosis kit (Annexin V-FITC, PI and binding buffer (BB)) and reactive oxygen species assay kit 2, 7-Dichlorodi-hydrofluorescein diacetate (DCFH-DA) were obtained from Beyotime Co., Ltd.

Instruments

The morphologies of samples were characterized on a JEM-2100 plus (Japan) transmission electron microscope (TEM) and high-resolution TEM (HRTEM) with a voltage of 200 kV. Atomic force microscope (AFM) images were taken by a Veeco Nanoscope Quadrex AFM (Bruker, Germany). The photoluminescence (PL) spectra and absolute quantum yield (QY) of OR-CDs were tested by a time-resolved and

steady state fluorescence spectrometer Horiba JobinYvon FluoroMax 4C-L (France). Fluorescence lifetimes of OR-CDs were obtained on ultrafast time-resolved fluorescence lifetime spectrometer FL 980 (Lifespec ll, Edinburgh Instruments). Femtosecond transient absorption (fs-TA) spectra of R-CDs were carried out at 400 nm excitation, and the setup was provided by the Dalian Institute of Chemical Physics, Chinese Academy of Science. UV-vis absorbance spectra were measured by UV-3600 spectrophotometer (Shimadzu, Kyoto, Japan). Fourier transform infrared (FT-IR) spectra were recorded by an infrared spectrophotometer (Thermo Fisher Scientific, USA). The dynamic light scattering (DLS) and zeta potential were measured by a nano particle size analyzer (Zeta PALS, Brookhaven, USA). Thermal stability property of OR-CDs was analyzed by thermogravimetric (TGA) analyser under N_2 atmosphere from 25 °C to 800 °C with the heating rate of 5 °C min^{-1} (Mettler Toledo, Switzerland). Differential scanning calorimetry (DSC) measurements were carried out on a thermogravimetric analysis (TA) instrument (New Castle, USA). X-ray photoelectron spectra (XPS) were measured by an X-ray photoelectron spectrometer with Al Kα (1486.6 eV) radiation. High performance liquid chromatography (HPLC) was conducted by a high pressure liquid chromatgraph (1525, Waters, USA), and the mobile phases are acetonitrile, water and methanol. Ultra-high performance liquid chromatography tandem quadrupole time-of-flight mass spectrometer (LC-MS) was used to identify the R-CDs in low molecular fractions (MALDI SYNAPT MS, Waters, USA). Cytotoxicity was evaluated on a full-function microplate detector (Synergy H4, China). The confocal microscopy images were collected using the confocal fluorescence microscope (Carl Zeiss LSM880). The apoptotic and necrotic cells were analyzed by a flow cytometer (BD Accuri C6 Plus USA). A LED hand lamp (yellow light, 0.088 W cm^{-2}) was used as the light source, which has a center wavelength at 590 nm (Kiwi Photoelectric Co., Ltd. Shenzhen, China).

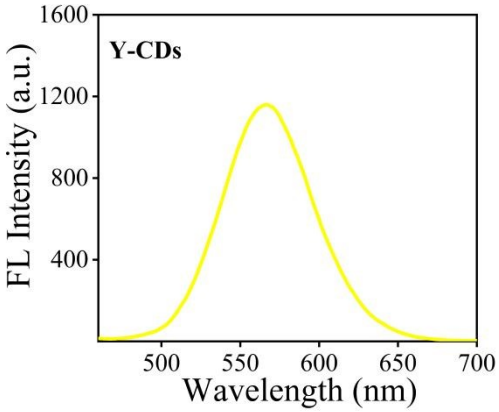

Fig. S1 The fluorescence spectra of Y-CDs, inset: Inset: the optical photographs of Y-CDs solution under daylight (left) and UV (365 nm, right).

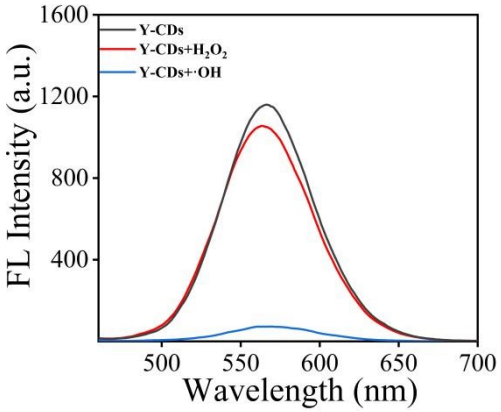

Fig. S2 The fluorescence spectra of Y-CDs in presence of ROS. Y-CDs were prepared from OPD and catechol by hydrothermal treatment at 180 °C for 5 h. ROS were added to Y-CDs solution, respectively, including 20 μM H_2O_2, or 20 μM ·OH.

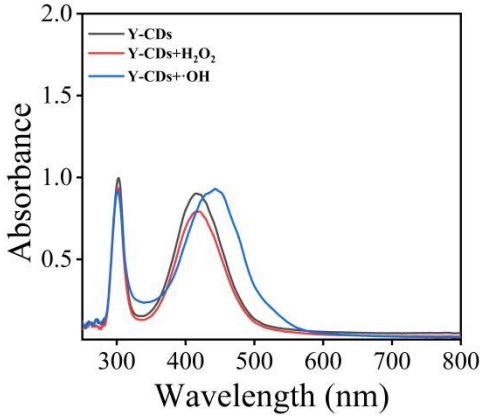

Fig. S3 The UV-vis absorbance spectra of Y-CDs in presence of ROS. Y-CDs were prepared from OPD and catechol by hydrothermal treatment at 180 °C for 5 h. ROS were added to Y-CDs solution, respectively, including 20 μM H_2O_2, or 20 μM ·OH.

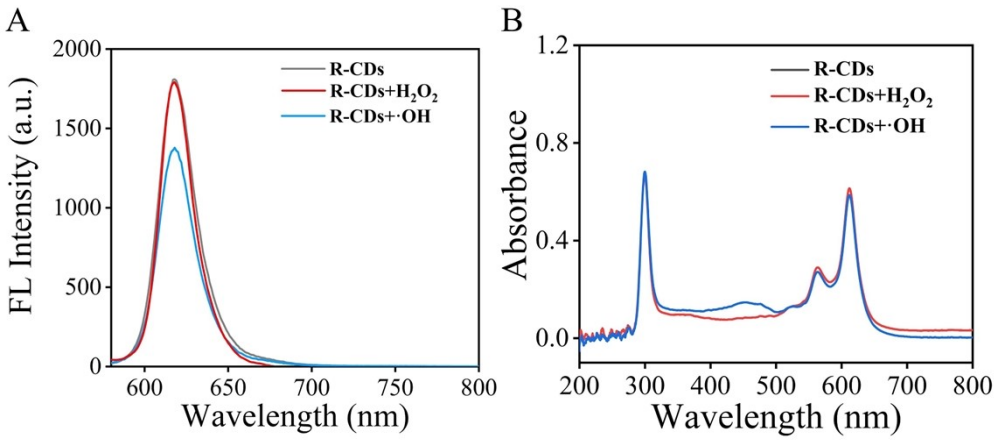

Fig. S4 (A) The fluorescence spectra of R-CDs in presence of ROS, which were prepared from Y-CDs by hydrothermal treatment H_3PO_4 at 180 °C for 1 h. ROS including 20 μM H_2O_2, 20 μM or ·OH were added to R-CDs solution, respectively. (B) The UV-vis absorbance spectra of R-CDs in presence of ROS, which were prepared from Y-CDs by hydrothermal treatment H_3PO_4 at 180 °C for 1 h. ROS including 20 μM H_2O_2, or 20 μM ·OH were added to CDs solution, respectively.

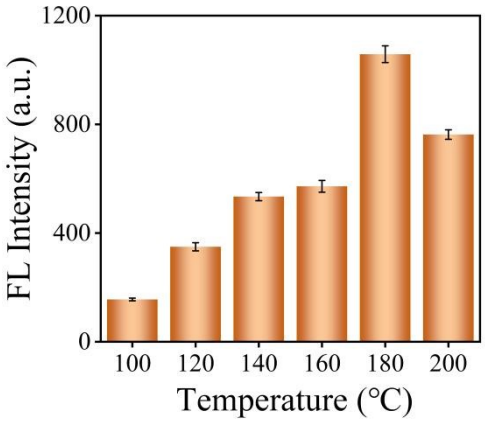

Fig. S5 Fluorescent intensity of the products prepared from different hydrothermal temperatures, inset: photograph of corresponding products under daylight.

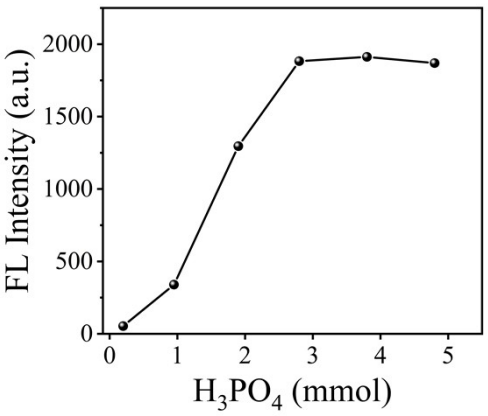

Fig. S6 The fluorescence intensity of the hydrothermal products obtained from adding different amounts of H_3PO_4 to they-CDs solution at 180 °C for 1 h.

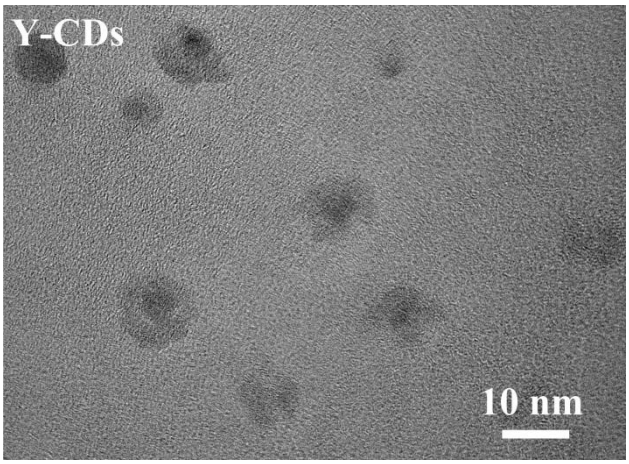

Fig. S7 HRTEM image of Y-CDs.

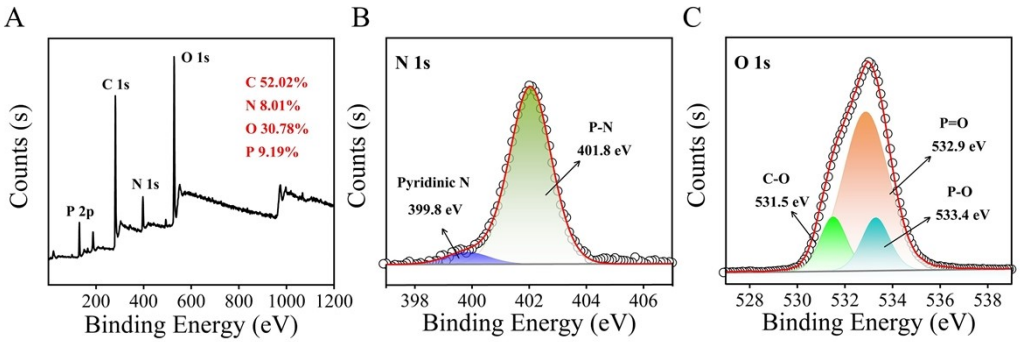

Fig. S8 (A) Survey of XPS spectrum of R-CDs (B-C) High-resolution XPS spectra of N 1s and O 1s for the R-CDs

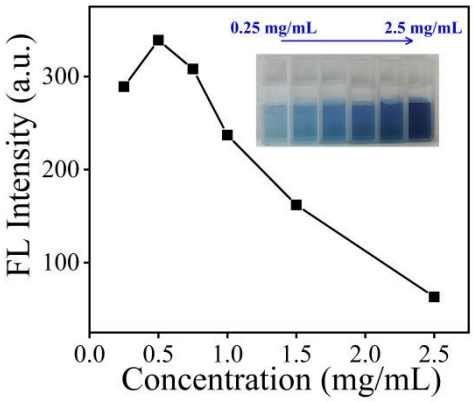

Fig. S9 Fluorescent intensities of different concentration R-CDs solutions, inset: the photographs of corresponding R-CDs solutions under daylight.

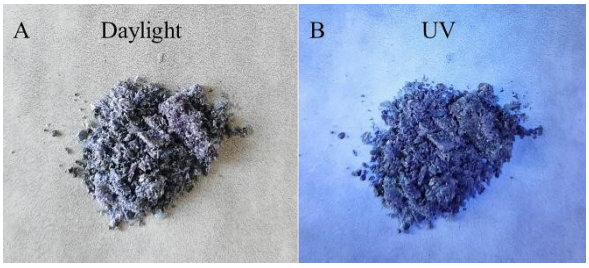

Fig. S10 Photos of R-CDs powders under (A) daylight and (B) UV light

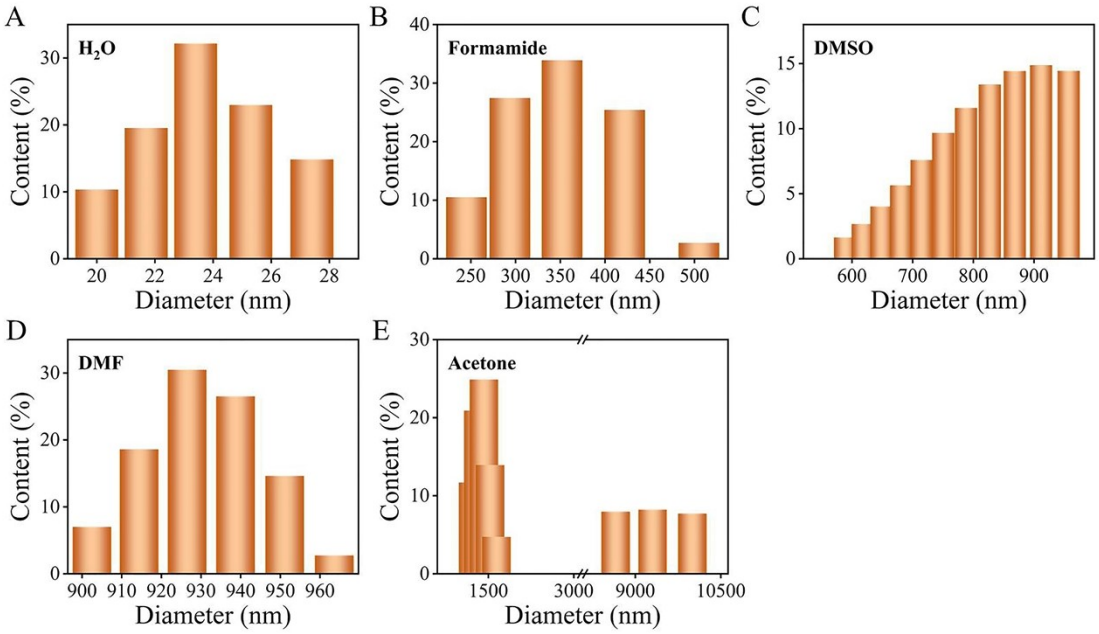

Fig. S11 The hydrodynamic diameters of 0.50 mg/mL R-CDs in different solvents determined by dynamic light scattering (DLS) (A) H_2O; (B) Formamide; (C) DMSO; (D) DMF; and (E) Acetone.

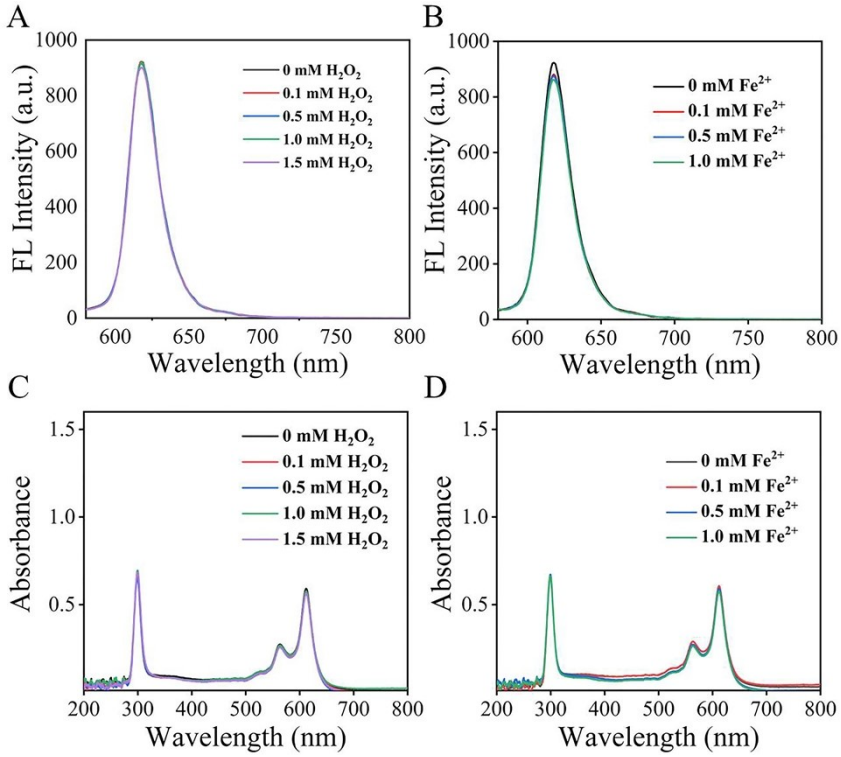

Fig. S12 (A) The fluorescence spectra of R-CDs in presence of different concentrations of H_2O_2. (B) The fluorescence spectra of R-CDs in presence of different concentration Fe^{2+}. (C) The UV-vis absorbance spectra of R-CDs in presence of different concentration H_2O_2. (D) The UV-vis absorbance spectra in presence of different concentration Fe^{2+}.

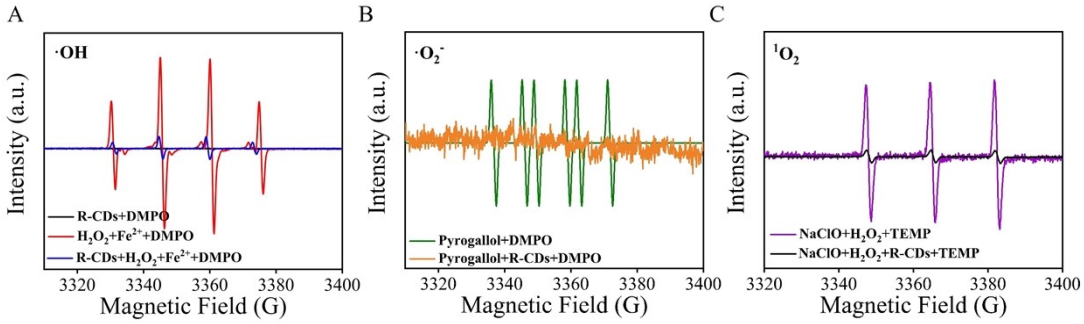

Fig. S13 ESR analysis: (A) ESR spectra of the samples containing DMPO, Fe^{2+}, H_2O_2 with and without R-CDs. (B) ESR spectra of the samples containing DMPO, pyrogallol with and without R-CDs. (C) ESR spectra of the samples containing DMPO, NaClO, H_2O_2 with and without R-CDs.

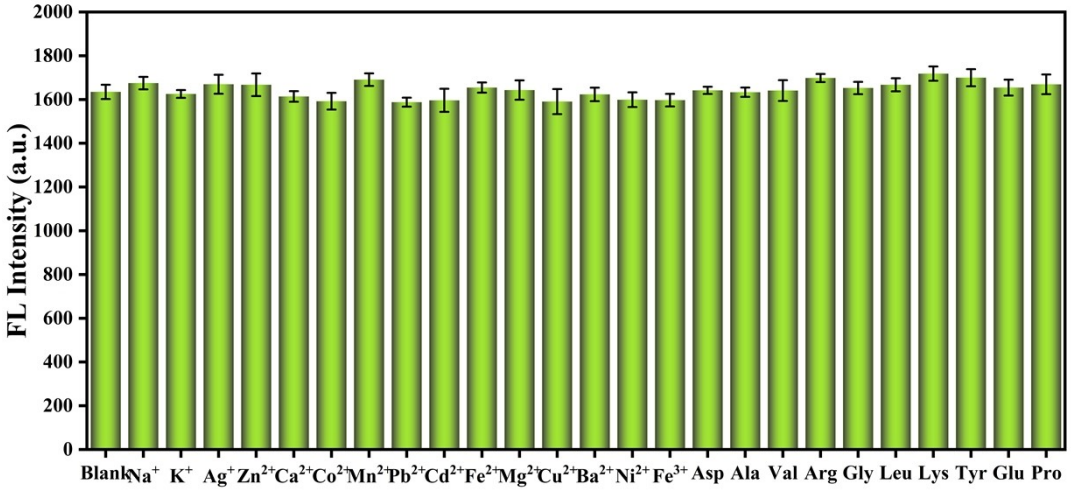

Fig. S14 Influence of metal ions and biomolecules on the fluorescence intensity of the 0.5 mg/mL R-CDs. The test metal ions or biomolecules include 20 μM Na^+, K^+, Ag^+, Zn^{2+}, Ca^{2+}, Co^{2+}, Mn^{2+}, Pb^{2+}, Cd^{2+}, Fe^{2+}, Mg^{2+}, Cu^{2+}, Ba^{2+}, Ni^{2+}, Fe^{3+}, aspartic acid (Asp), alanine (Ala), valine (Val), arginine (Arg), glycine (Gly), leucine (Leu), lysine (Lys), tyrosine (Tyr), glutamic acid (Glu), or proline (Pro).

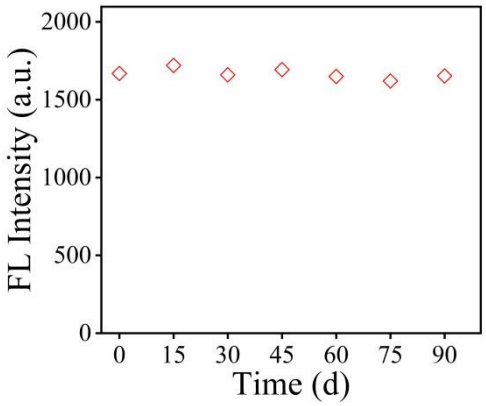

Fig. S15 Fluorescence intensity of R-CDs solution stored different time.

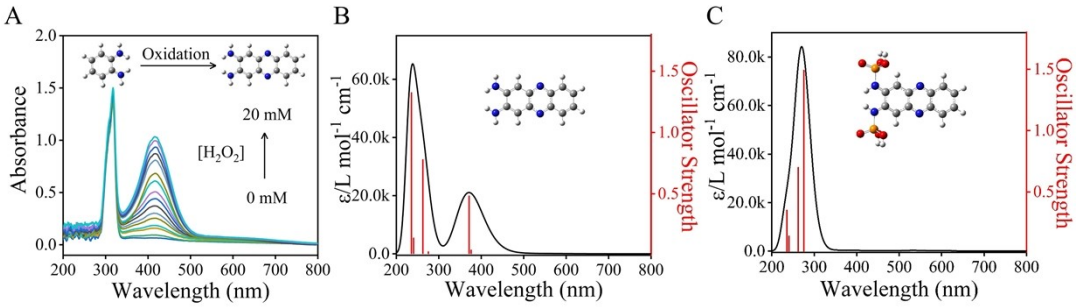

Fig. S16 (A) The UV-vis absorbance spectra during the oxidation of o-phenylenediamine by H_2O_2, (The concentration of o-phenylenediamine is 1.0 mM; the concentration of H_2O_2 is ranging from 0 to 20 mM). (B) The DFT calculated UV-vis absorbance spectrum of 2, 3-diaminophenazine. (C) The UV-vis absorbance spectra during the 2, 3-diaminophenazine protected by phosphate groups.

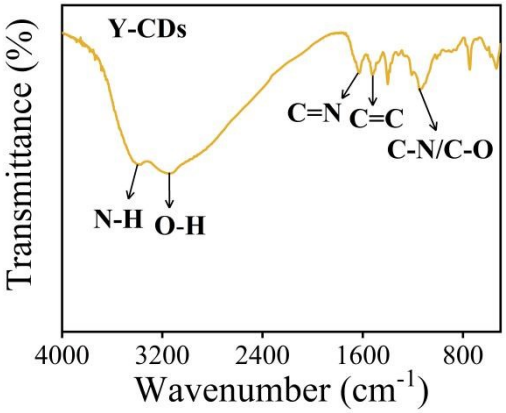

Fig. S17 The FT-IR spectra of Y-CDs.

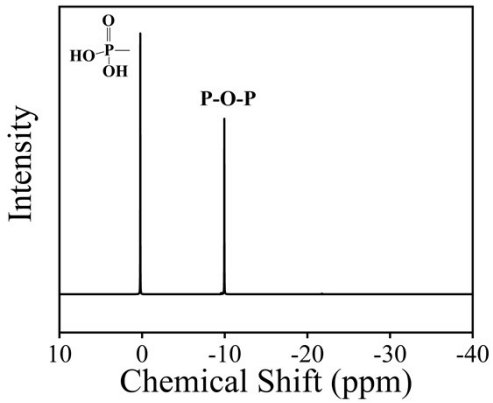

Fig. S18 The ^{31}P NMR spectrum of R-CDs

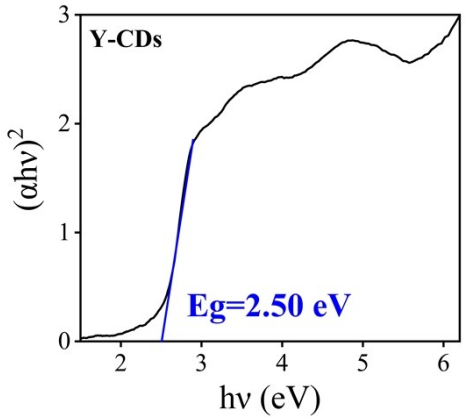

Fig. S19 Plot of $(\alpha h\nu)^2$ versus $(h\nu)$ for the band gap energy of Y-CDs

The band gap energy (Eg) values of all optimized geometries can be estimated from the DRS by using the formula:[1]

$$\alpha h\nu = K(h\nu - Eg)^n$$

Where α refers to the absorption coefficient, hν is the energy of the incident light, Eg is the energy gap and n is a number which characterizes the optical absorption processes.

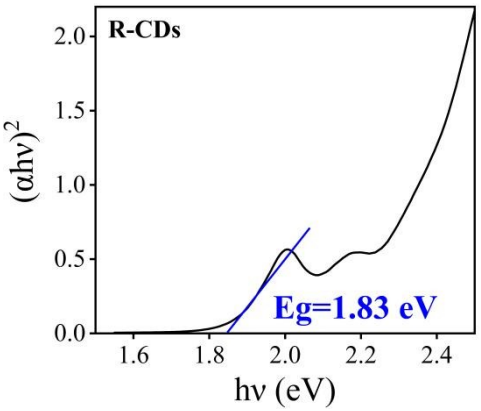

Fig. S20 Plot of $(\alpha h\nu)^2$ versus $(h\nu)$ for the band gap energy of R-CDs

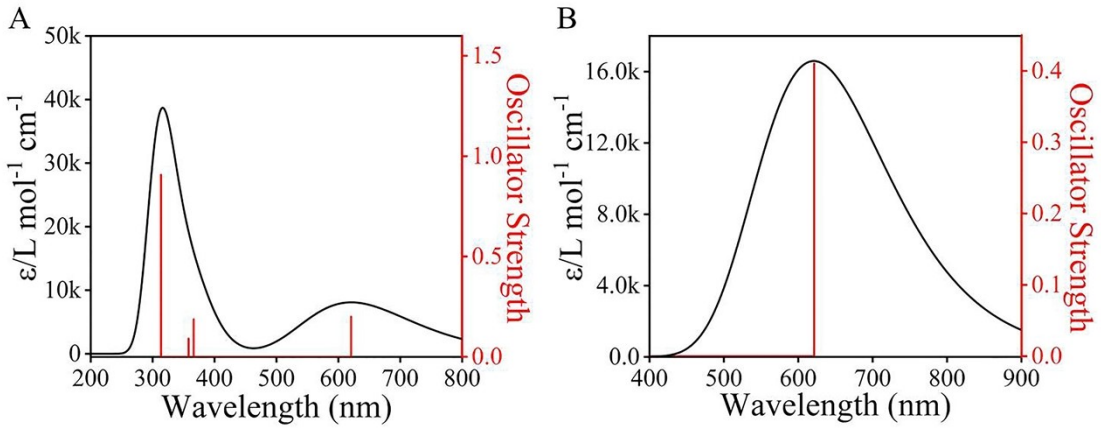

Fig. S21 (A) The calculated absorption spectrum of R-CDs (B) The calculated fluorescence spectrum of R-CDs

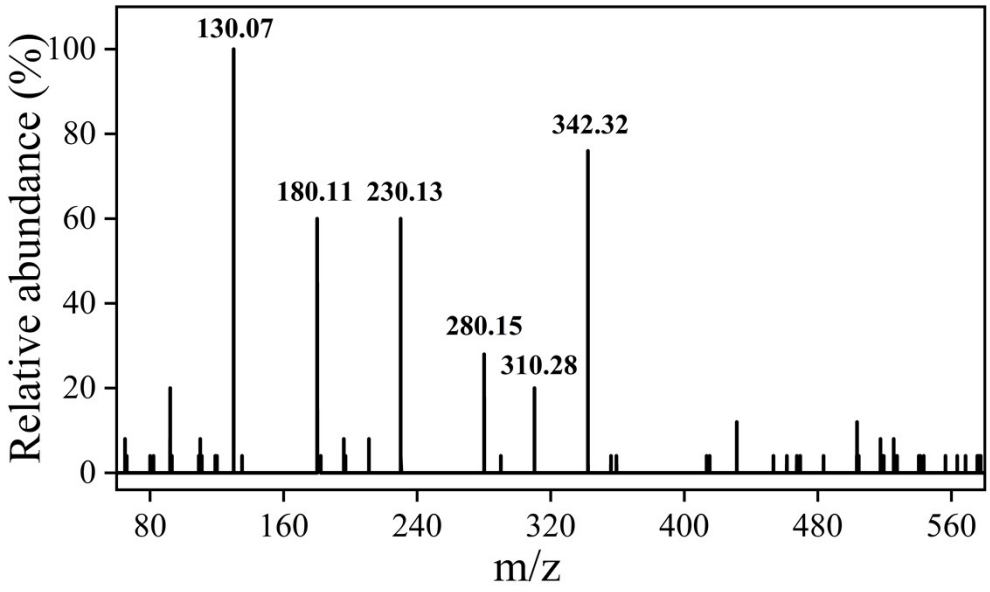

Fig. S22 Mass spectrum of Y-CDs

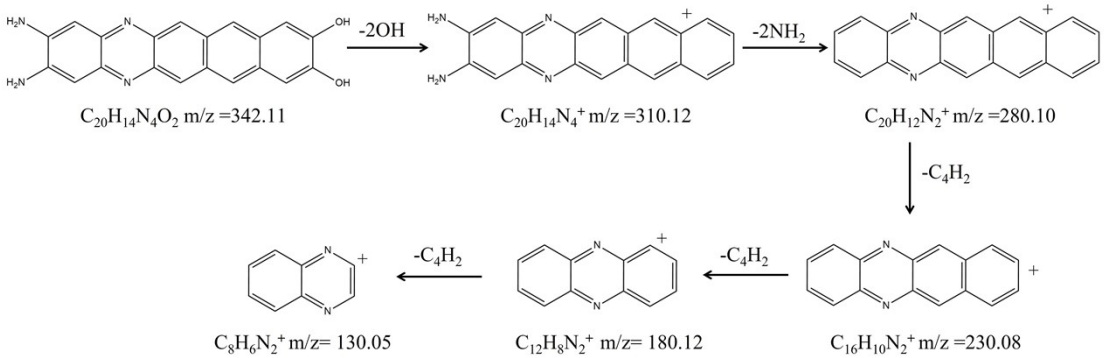

Fig. S23 The proposed decomposition process of Y-CDs

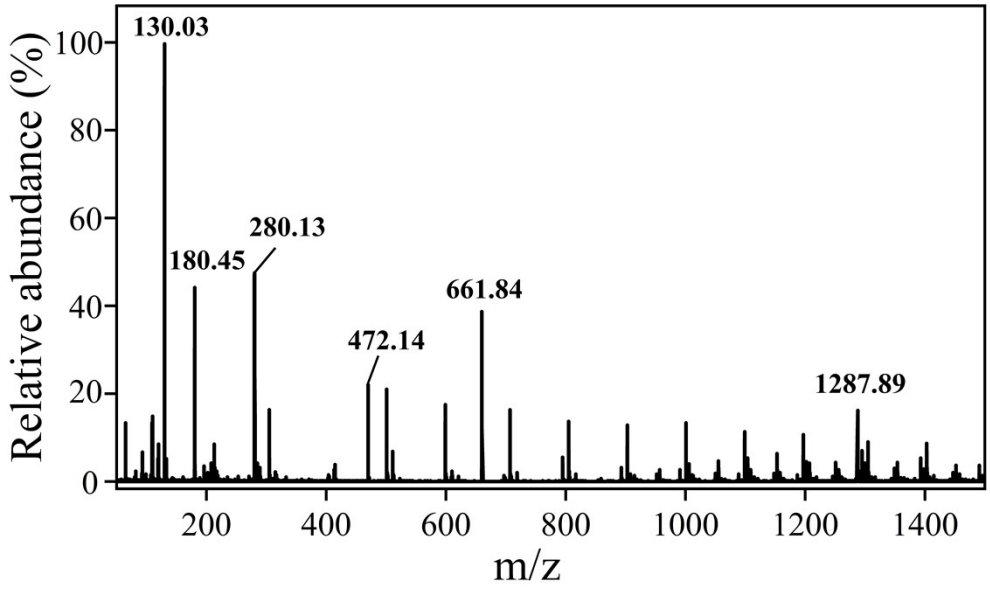

Fig. S24 Mass spectrum of R-CDs

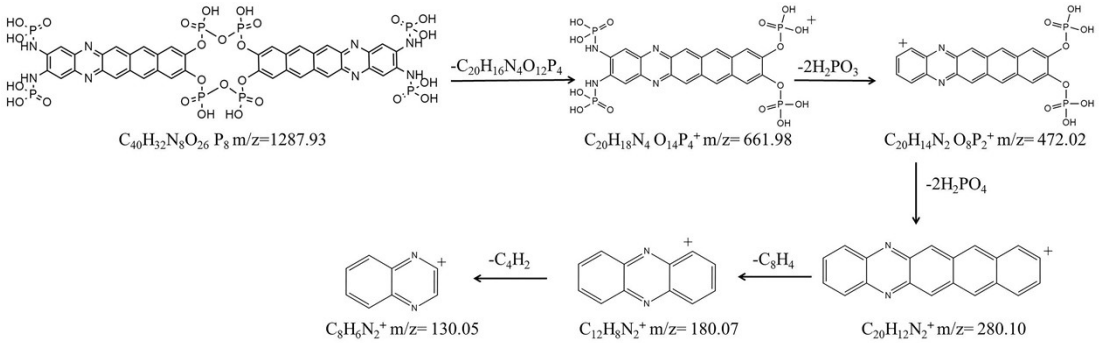

Fig. S25 The proposed decomposition process of R-CDs

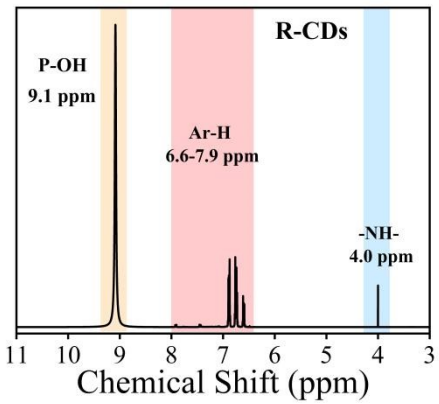

Fig. S26 The ^{1}H-NMR spectrum of R-CDs in DMSO-d6

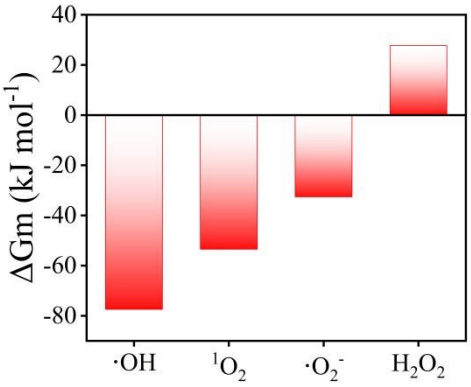

Fig. S27 Theoretically calculated ΔGm of the reaction between R-CDs and ·OH, $^{1}O_2$, $\cdot O_2^-$, and H_2O_2, respectively.

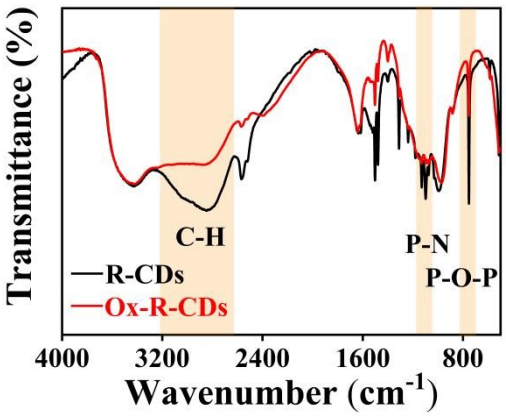

Fig. S28 The FT-IR spectra of R-CDs and Ox-R-CDs

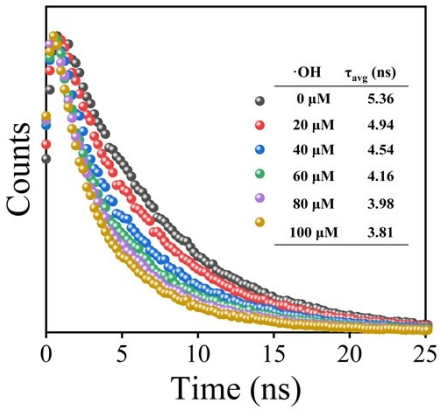

Fig. S29 Lifetime decays of R-CDs with different concentration ·OH

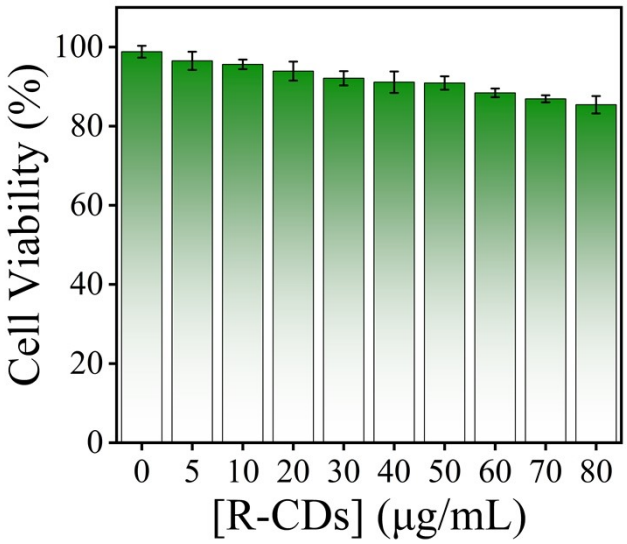

Fig. S30 Viability of A549cells incubated with different concentrations of R-CDs for 12 h.

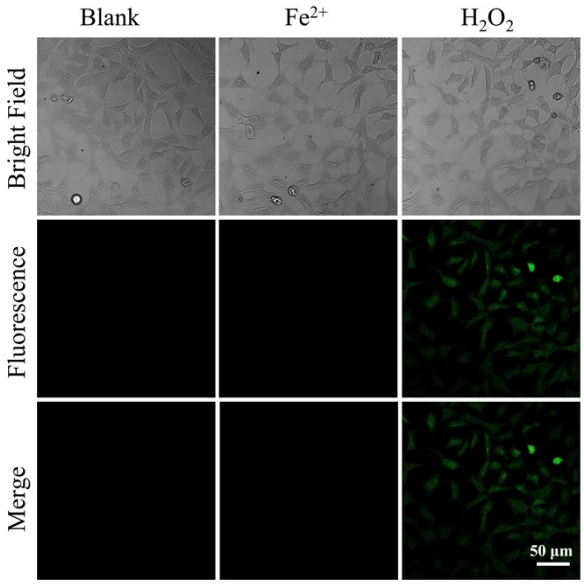

Fig. S31 Confocal fluorescence images of A549 cells. The scale bar is 50 μm. Three groups of A549 cells are respectively untreated, treated with 20 μM Fe^{2+} or treated with 10 μM H_2O_2.

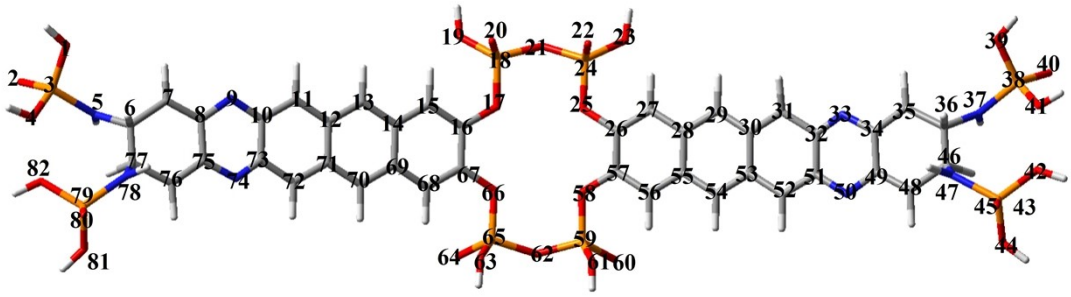

Fig. S32 The structure of basic unit **5**c-O/O-**5**c

The two 5-member aromatic units are the basic unit of R-CDs, i.e., **5**c-O/O-**5**c, whose atoms are numbered, except for hydrogen (Fig. S32). The distance between atoms was estimated in Gauss View 5.0. As shown in Table S2, the distance between the atoms in **5**c-O/O-**5**c is ranging from 0.13 to 3.31 nm. According to TEM image in Fig. 1C, R-CDs exhibit good uniform dispersion of ca. 3.02 nm ranging from 2.15 to 4.25 nm quasi-spherical nanoparticles, and Fig. 1D illustrates that the R-CDs possess a narrow size distribution with an average height ca. 2.68 nm. Therefore, we tentatively concluded that the **5**c-O/O-**5**c basic units may be stacked in the R-CDs.

Table S1 HOMO and LUMO energies and corresponding E_g values of the twenty one optimized structures.

	HOMO (eV)	LUMO (eV)	Eg (eV)
3	-3.32	0.42	3.74
4-1	-3.37	-0.38	2.99
4-2	-2.32	0.73	3.05
4-3	-2.69	0.29	2.98
5-1	-4.34	-1.72	2.62

5-2	-4.49	-1.99	2.50
4a	-2.38	1.02	3.40
4b	-4.03	-1.45	2.58
4c	-5.86	-3.09	2.77
4d	-2.89	0.04	2.93
4e	-3.09	-0.13	3.22
4f	-5.99	-3.25	2.74
4g	-3.16	-1.19	1.97
5a	-3.07	-0.51	2.56
5b	-3.18	-0.31	2.87
5c	-3.16	-1.26	1.90
5d	-4.12	-1.77	2.35
5e	-3.47	-1.92	1.55
5f	-3.63	-1.35	2.28
5g	-4.02	-1.95	2.07
5h	-3.11	-1.48	1.63

Table S2 The distance between atoms of **5**c-O/O-**5**c

Atomic number	**length (Å)**	**length (nm)**
1→23	19.0	1.90
1→39	30.1	3.01
1→42	31.7	3.17
1→45	30.7	3.07
1→81	6.6	0.66
1→20	14.3	1.43
2→42	33.1	3.31
2→81	6.2	0.62
3→38	31.3	3.13
3→43	30.9	3.09
3→79	4.4	0.44
5→37	28.6	2.86
5→47	27.9	2.79
5→78	3.1	0.31
7→76	2.7	0.27

8→75	1.3	0.13
19→23	5.4	0.54
19→44	20.0	2.00
19→63	7.6	0.76

References

1. S. Chandra, P. Patra, S. H. Pathan, S. Roy, S. Mitra, A. Layek, R. Bhar, P. Pramanik and A. Goswami, *J. Mater. Chem. B*, 2013, **1**, 2375-2382.